PCCP

Accepted Manuscript

ROYAL SOCIETY OF CHEMISTRY

www.rsc.org/pccp

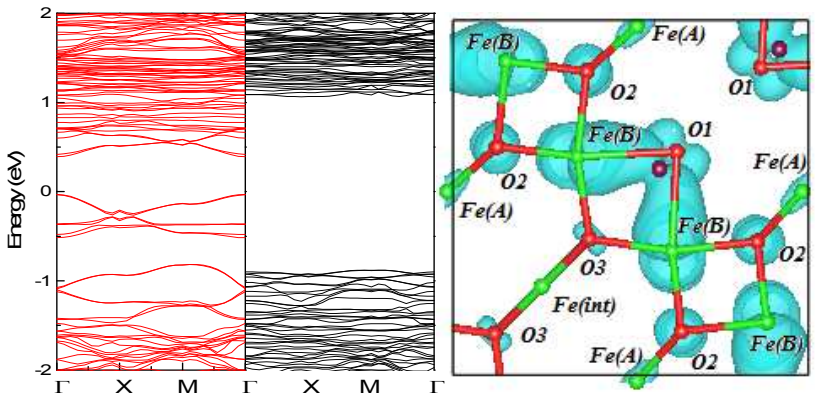

Spin polarization of the Fe3O4(100) surface is enhanced by B adsorption through the opening of the spin-up band gap.

Half-Metallicity Induced by Boron Adsorption on an $Fe_3O_4(100)$ Surface

X. Sun[1,2], A. Pratt[2,3], and Y. Yamauchi[2]

1. Key Laboratory of Strongly-Coupled Quantum Matter Physics, Chinese Academy of Sciences, School of Physical Sciences, University of Science and Technology of China, Hefei, Anhui 230026, China

2. National Institute for Materials Science, 1-2-1 Sengen, Tsukuba, Ibaraki 305-0047, Japan

3. Department of Physics, University of York, Heslington, York YO10 5DD, U.K.

The spin polarization of magnetite Fe_3O_4 is significantly reduced at its surfaces, which is unfavorable for the development of spintronic devices based on this material. In order to enhance the surface spin polarization, the $Fe_3O_4(100)$ surface is modified here through the adsorption of boron (B) atoms and investigated by density functional theory (DFT) calculations. We find for the bulk-terminated and cation-redistributed surfaces that a band gap is opened in the spin-up electronic states due to the formation of a strong bond between the B atom and a surface oxygen atom, i.e., B adsorption induces half-metallicity at the Fe3O4(100) surface. Besides the surface Fe and O atoms, the adsorbed B atoms have a considerable density of -100% spin-polarized electronic states at the Fermi level, which might provide a means to improving the efficiency of spin injection in spintronic devices.

I. Introduction

Half-metallic materials have huge potential in spintronic applications due to an extreme spin polarization at the Fermi level (P_{EF} =100% or -100%). Half-metallicity has theoretically been predicted to occur in the bulk of magnetite Fe_3O_4 [1] and was recently characterized, through femtosecond spin excitation, by a long demagnetization time that is two orders of magnitude higher than for Ni.[2] Another advantage of Fe_3O_4 is its exceptionally high Curie temperature of 860 K.[1] Instead of conventional ferromagnetic metals (e.g. Fe, Co, Ni, etc.), Fe_3O_4 is now widely investigated as a magnetic substrate for the injection of spin-polarized

current into nonmagnetic materials. For example, magnetic tunnel heterojunctions have been fabricated through thermal evaporation of DITPY on an Fe_3O_4 (111) thin film,[3] whilst layers of Alq_3,[4] C60,[5] FePc [6] and C_6H_6 [7] have been successfully deposited onto Fe_3O_4 (111) and (100) surfaces. Nanoparticles of Fe_3O_4 have also been used as a magnetic core in core-shell structures wrapped with polymethylmethacrylate (PMMA),[8] oleic acid,[9] polyaniline,[10] gold,[11] and single-walled carbon nanotubes.[12] Practical spintronic devices naturally require the presence of at least one interface, however, it has been conclusively shown that the half-metallicity is not maintained at the surface of Fe_3O_4. Reduced P_{EF} values of $-(55\pm10)\%$ (Fonin *et al.* [13]) and -40% (Tobin *et al.* [14]) have been observed for the $Fe_3O_4(100)$ surface at room temperature using spin-resolved photoemission spectroscopy (SPPES) and reproduced by theoretical calculations using density functional theory (DFT).[15,16] Therefore, an improvement in the surface spin polarization is crucial for the development of Fe_3O_4-based spintronic devices.

To this end, an enhancement in P_{EF} has been observed for the H-adsorbed $Fe_3O_4(100)$ surface using spin-polarized metastable deexcitation spectroscopy (SPMDS) and SPPES.[17-19] DFT calculations confirm that half-metallicity is recovered through quenching of oxygen dangling bonds at the surface.[15,19] Recently, the adsorption of carbon has also been theoretically predicted to recover half-metallicity at the $Fe_3O_4(100)$ surface with a wider spin-up band gap than for H-adsorption.[20] However, extremely high temperatures (>3500 $^{\circ}$C) are needed to deposit atomic carbon making this system very difficult to realize experimentally. In similarity with C atoms, B atoms form strong bonds with surface O atoms but the temperature required for atomic B adsorption is much lower than for C, hence, a B-adsorbed surface should be easier to achieve experimentally. In this study, we have investigated the B-adsorbed $Fe_3O_4(100)$ surface by DFT calculations, and compared the corresponding result with that of the H-adsorbed and C-adsorbed $Fe_3O_4(100)$ surface. Our calculations predict that the half-metallicity can also be induced or recovered by B adsorption with a spin-up gap wider than that for H adsorption and very close to that for C adsorption. Adsorbed H atoms have no electronic density at the Fermi level. On the contrary, adsorbed C and B atoms have some electronic density of states (DOS) with -100% P_{EF}, where the Fermi level DOS of the adsorbed B atom is larger than that of the adsorbed C atom. This might be helpful to improve the efficiency of spin injection in spintronic devices.

II. Calculation methods

All calculations were performed within the framework of DFT using a plane-wave basis set, as implemented in the Vienna *ab initio* simulation package (VASP).[20,21] The calculation model and parameters are similar to those in our previous study of H adsorption on the Fe_3O_4(100) surface.[15] Exchange-correlation interactions are described by the Perdew-Burke-Ernzerhof-generalized gradient approximation (GGA).[22] The projector-augmented wave method is used to represent the electron-ion interaction.[24,25] The Brillouin-zone integration is calculated with a 4×4×1 *k*-point grid using the Monkhorst-Pack method.[26] All calculations are spin-polarized with a 400 eV plane-wave energy cutoff. A reconstructed substrate is used with a $\left(\sqrt{2}\times\sqrt{2}\right)R45^{o}$ unit cell, which has been observed by low energy electron diffraction (LEED)[13,16] as well as scanning tunneling microscopy (STM) [27] and reproduced by DFT calculations.[13,16,28] The surface is represented by a 13-layer slab with both sides terminated by octahedral Fe(B) atoms, which is energetically more favorable than a surface terminated by tetrahedral Fe(A) atoms.[29,30] The vacuum region is as large as 17.5 Å. B atoms are adsorbed on the topmost and bottom-most surfaces. All adsorbed and substrate atoms are relaxed until the force on each atom is less than 0.01 eV/ Å.

III. Results and Discussion

For the Fe(B)-terminated Fe_3O_4(100) surface, there are two kinds of surface oxygen atom, denoted by O1 (with no tetrahedral Fe(A) neighbor) and O2 (with an Fe(A) neighbor) in the following text. As for H and C atoms, B atoms preferentially bond to O1 atoms with an adsorption energy (-5.761 eV) that is significantly larger than for H adsorption (-3.096 eV), and slightly larger than for C adsorption (-5.509 eV). Here, the adsorption energy is defined as $E_{ads} = (E_{nB/Fe_3O_4(100)} - E_{clean-Fe_3O_4(100)} - nE_B)/n$, where n is the number of adsorbed B atoms, and $E_{nB/Fe_3O_4(100)}$, $E_{clean-Fe_3O_4(100)}$ and E_B are the total energies of the B-adsorbed surface, the clean Fe_3O_4(100) surface and a free B atom, respectively. Strong chemisorption leads to a tilted geometry of the B-O1 bond with a tilting angle of 57.9° from the surface normal, and a short bond length of 1.303 Å (Table 1). The green and red spheres in Fig. 3 represent Fe(B) and O atoms located at the topmost layer of the substrate with gray, brown and purple spheres indicating the respective positions of adsorbed H,

C and B atoms. B adsorption leads to an acute angle of Fe(B)-O1-B bond formation (72°) that is much less than the more obtuse Fe(B)-O1-H bond (122.6°) formed upon H adsorption. This difference in the adsorption geometry is caused by the demand of total energy minimization for each adsorption. Chemical adsorption also induces considerable surface modification, which can be observed from the change in distance between nearest neighboring atoms such as for O1-O1, O2-O2, Fe(B)-O1, Fe(B)-Fe(B), etc. (see Table 1). Such modification results in an increase of the total energy of the Fe_3O_4(100) surface, which is obviously larger for B adsorption (+1.121 eV) than for H adsorption (+0.609 eV). The surface modification energy is calculated as $E_{surf} = (E_{\mathrm{mod}-Fe_3O_4(100)} - E_{clean-Fe_3O_4(100)})/n$, where $E_{\mathrm{mod}-Fe_3O_4(100)}$ is the total energy of the modified Fe_3O_4(100) surface which has the same geometric structure as the adsorbed system. On the other hand, the total energy is decreased by the adsorbate-substrate interaction and the adsorbate-adsorbate interaction. The nearest B-B distance and Fe(B)-B distance will be smaller for a geometry with an obtuse Fe(B)-O1-B angle than for those with a more acute angle, indicating stronger adsorbate-adsorbate and adsorbate-substrate interactions. Our calculation shows that for a B-adsorbed surface, the decrease in energy due to the B-B interaction (-1.844 eV) is considerable and enough to compensate for the increase in energy caused by the large surface modification (+1.121 eV). Here, the B-B interaction energy is calculated as $E_{B-B} = (E_{nB} - nE_B)/n$, where E_{nB} is the total energy of the adsorbates considering a set of *n*-adsorbed B atoms with the same geometric structure of the adsorption system. As shown in Table 1, the nearest Fe(B)-B distance (2.266 Å) has the same value as for Fe(B)-O1 at the geometry with an acute Fe(B)-O1-B angle, indicating that the Fe(B)-B interaction can not be negligible and will furthermore induce a considerable decrease of the total energy. As for H adsorption, the H-H and Fe(B)-H interactions are much weaker than for B-B and Fe(B)-B. The total energy will not be significantly reduced even when considering the same geometry as for B adsorption because of the smaller atomic radius and number of valence electrons of H. Therefore, H preferentially adsorbs with a geometry leading to an obtuse Fe(B)-O1-H bond angle as this arrangement results in a smaller surface modification. In contrast, the large increase (+1.812 eV) in the total energy of the Fe_3O_4(100) surface for C adsorption is mediated mainly by the large C-substrate interaction energy (-6.240 eV) and not the small C-C interaction energy (-1.081 eV). Here, the direct interaction energy between adsorbate and substrate is calculated as

$E_{M-sub} = E_{nM/Fe3O4} - E_{\mathrm{mod}-Fe3O4} - E_{nM} = E_{ads} - E_{surf} - E_{M-M}$, which has excluded effects due to surface modification and adsorbate-adsorbate interactions. As for B adsorption, the large C-substrate interaction induces an acute angle of Fe(B)-O1-C (82.5°C).

Figure 1 shows the spin-resolved band structure and total DOS of the B-adsorbed Fe_3O_4(100) surface. A band gap is opened in the spin-up electronic states by B adsorption (left panel) leading to a surface that becomes half-metallic with -100% spin polarization of electronic states at the Fermi level (right panel). Previous studies[15,19] show that H and C adsorption also result in an opening of the spin-up gap and a recovery of the half-metallicity of the Fe_3O_4(100) surface. However, in comparison with H adsorption, there are some obvious superior aspects of B adsorption. The first one is the energy range of the available half-metallic states. The band gap ($\Delta_{\text{spin-up}}$) of spin-up electronic states (0.74 eV) is larger than for the H-adsorbed surface (0.65 eV) and closer to that of the bulk (0.87 eV). The energy interval ($\Delta_{\text{EF-VBM}}$) from the Fermi level to the valence band maximum (VBM) is also wider for the B-adsorbed surface (0.37 eV) than for the H-adsorbed one (0.25 eV). All the spin-up surface state bands (SSB) that are present at the clean Fe_3O_4(100) surface[15] have been removed by the strong chemisorption of B atoms. In contrast, half of the SSB remain at the H-adsorbed Fe_3O_4(100) surface,[15] resulting in a narrower spin-up band gap. C-adsorption is also superior to H adsorption in terms of the spin-up band gap (0.73 eV).

Strong interaction between B and the substrate is reflected in the local DOS (Fig. 2). Peaks at -9.4, -8.0 and -7.6 eV in the O1 atom DOS (2nd panel of Fig. 2) are apparently induced by the adsorbed B atom through *s*-*s* and *s*-*p* hybridization. The induced peaks can also be observed in the Fe(B) atom DOS at the same energy positions (bottom panel of Fig. 2). A similar phenomenon occurs in the Fe(B) atom DOS for the H-adsorbed surface and has been attributed to a donation-redistribution mechanism, that is, electrons are donated from the adsorbate (H atom) to the O1 atom and then redistributed to the Fe(B) atom via the O1-Fe(B) bond.[15] Here, the density of the induced peaks in the Fe(B) atom DOS for the B-adsorbed Fe_3O_4 surface is found to be 1.5 times larger than for the H-adsorbed surface. The increase of the density is caused by an additional donation process through the direct interaction between Fe(B) and B atoms. For the H-adsorbed surface, the interaction between Fe(B) and H atoms might be negligible due to the length of Fe(B)-H bond (2.762 Å) and the small atomic radius of the H atom. Besides the induced states at deep

levels, the electronic states of B-2*p* overlap with those of O1-2*p* and Fe(B)-3*d* in a wide energy range below the Fermi level (Fig. 2), indicating significant *p*-*p* and *p*-*d* hybridization. Consequently, all SSB are removed by the strong B-substrate interaction and a spin-up gap is opened to recover the half-metallicity.

Magnetite films are being investigated as magnetic electrodes for the injection of spin-polarized current into nonmagnetic materials such as organic films in spintronic devices.[3-7] In this sense, it is important to have more atoms which could provide spin-polarized states with a high density and large P_{EF}. Fig. 3 shows the spin density of the topmost surface for clean, H-adsorbed, C-adsorbed and B-adsorbed Fe_3O_4(100) surfaces. Considering the energy resolution of experiments that probe the surface DOS, the spin density is integrated from -0.5 eV to the Fermi level. The isosurface plotted with yellow and blue represents positive and negative spin density, respectively. For the clean Fe_3O_4(100) surface (Fig. 3(a)), the spin density is positive in all surface O1 and O2 atoms as well as in the d_{x2-y2} orbital of Fe(B) atoms. Negative spin density can only be observed in the d_{xz}/d_{yz} orbital of Fe(B) atoms. Therefore, due to the dominant positive density, the spin density integrated over the entire area of the topmost surface is greatly decreased, corresponding well to the reduced P_{EF} observed experimentally.[13,14] For the H-adsorbed Fe_3O_4(100) surface (Fig. 3(b)), the spin density is still positive in all O1 and O2 atoms, however, with a lower density in O1 atoms. This is due to the fact that spin-up SSB with charge density of O1 atoms along [110] directions have been shifted to a deeper level by the formation of H-O1 bonds.[15] The positive spin density in the d_{x2-y2} orbital of Fe(B) becomes insignificant also due to the removal of half of the SSB. The dominant spin density of Fe(B) is negative and arises from the d_{xy} orbital. The density increase in the d_{xy} orbital is caused by the enhancement of the Fe(B)-Fe(B) interaction, indicated by a 0.35 Å decrease of the distance between Fe(B)-Fe(B) atoms due to H adsorption. For the C-adsorbed and B-adsorbed Fe_3O_4(100) surfaces (Fig. 3(c) and (d)), the spin density is negative not only in Fe(B) atoms but also in all O1 and O2 atoms because all spin-up SSB have been removed by the strength of C or B adsorption. Another important characteristic is that no spin density can be observed in the adsorbed H atoms (Fig. 3(b)) since there are no electronic states around the Fermi level. In contrast, a significant negative spin density appears in the adsorbed B atoms (Fig. 3(d)), corresponding to the prominent spin-down peak in the local DOS around the Fermi level (top panel of Fig. 2). Therefore, besides a wider spin-up gap, B adsorption is superior to H adsorption as it results in a larger number of spin-polarized atoms and a higher density with -100% P_{EF}. The density of the adsorbed B atoms

with -100% P_{EF} is even larger than for the C-adsorbed surface (Fig. 3(c)). So, in addition to being easier to realize experimentally, B adsorption is superior to C adsorption as it leads to a larger density of fully spin polarized (P=-100%) electronic states.

Recently, Bliem *et al*. proposed that $Fe_3O_4(100)$ has a subsurface cation vacancy (SCV), as determined using a combination of quantitative low-energy electron diffraction (LEED), scanning tunneling microscopy (STM) and DFT calculations.[31] Here, the effect of B adsorption on surface spin polarization is furthermore investigated based on this SCV structure. The SCV structure is formed by replacing two Fe(B) atoms from the third layer by an interstitial Fe atom, denoted by Fe(int), with tetrahedral coordination in the second layer— a net removal of one cation per $\sqrt{2}\times\sqrt{2}$ unit cell.[31] Therefore, there are only two O1 atoms due to the appearance of the Fe(int) atom in the second layer. This modification yields an adsorption energy for a B atom of -5.657 eV which is slightly smaller than for the $Fe_3O_4(100)$ surface without the SCV (-5.761 eV). The B-O1 bond is also tilted with a tilting angle of 28.3° from the surface normal and a short bond length of 1.270 Å. In similarity to the B-adsorbed $Fe_3O_4(100)$ surface without the vacancy, a band gap (0.78 eV) is opened in the spin-up electronic states for the SCV structure (left panel in Fig. 4) and the spin polarization at the Fermi level is -100% (right panel in Fig. 4).

Calculations including the on-site Coulomb interaction (U) term for treating strong electron-correlation effects has proven to be successful in the prediction of the SCV structure of the $Fe_3O_4(100)$ surface.[31] In this study, we also conducted the calculation with the GGA+U method with U_{eff}= 3.8 eV. Compared with the GGA calculation, GGA+U yields a slight increase in the B–O1 bond length by 0.002 Å and decreases the B–Fe(B) bond length by 0.045 Å. The tilting angle of B–O1 decreases by 1.8°. The above means that the variation of geometric structure related to the adsorbate is insignificant. Similar behavior has been observed for the C-adsorbed $Fe_3O_4(100)$ surface.[20] Using the GGA+U method, the adsorption energy (-5.323 eV) is smaller than when using the GGA method, whereas the gap in the spin-up electronic states (1.99 eV) is obviously enlarged (left panel in Fig. 5a). A gap is also opened for the spin-down electronic states (middle panel in Fig. 5a) with six bands located at an energy just below the Fermi level. The spin density integrated from -0.5 eV to the Fermi level (Fig. 5b) is negative for all atoms on the topmost surface, as for B-adsorbed $Fe_3O_4(100)$ surface without the SCVs. The main difference is the orbital contributed to

the spin density. For the B-adsorbed SCV Fe_3O_4(100) structure, the orbitals are d_{yz} /d_{z2} of Fe(B), p_x/p_y of O1, p_z of O2 and p_x/p_y of O3 (surface oxygen atoms with an Fe(int) neighbor). Consequently, both the GGA and GGA+U calculations show that the enhancement of the spin polarization of the Fe_3O_4(100) surface through B adsorption is not changed by the SCV structure.

IV. Conclusion

Surface modification through B adsorption on the Fe3O4(100) surface has been investigated using DFT calculations for the bulk-terminated and cation-redistributed surfaces. In both cases, the degree of spin polarization of the Fe3O4(100) surface is enhanced by B adsorption through the opening of the spin-up band gap and recovery of half-metallicity. The B-modified Fe_3O_4(100) surface should lead to superior spin injection into nonmagnetic materials due to the appearance of a wide spin-up band gap, the large total number of spin-polarized atoms, and the high density of states around the Fermi level with a spin polarization of P_{EF} = -100%.

Acknowledgements

This work was supported by the National Basic Research Program of China (973 Program) under Grant No. 2012CB933702, the Natural Science Foundation of China under Grant Nos. 11179008, 90921013, and 11274284.

References

[1] Z. Zhang and S. Satpathy, Phys. Rev. B **44**, 13319 (1991).

[2] G. M. Muller, J. Walowski, M. Djordjevic, G. Miao, A. Gupta, A. V. Ramos, K. Gehrke, V. Moshnyaga, K. Samwer, J. Schmalhorst, A. Thomas, A. Hutten, G. Reiss, J. S. Moodera and M. Munzenberg, Nature Materials **8**, 56 (2009).

[3] S. Berny, L. Tortech, D. Fichou, S. Matzen, and J.-B. Moussy, Appl. Phys. Lett. **97**, 253303 (2010).

[4] E. Arisi,I. Bergenti, M. Cavallini, A. Riminucci, G. Ruani, V. Dediu, M. Ghidini, C. Pernechele, and M. Solzi， Appl. Phys. Lett. **93**, 113305 (2008).

[5] P. K. J. Wong, W. Zhang, K. Wang, G. van der Laan, Y. Xu, W. G. van der Wiel and M. P. de Jong, J. Mater. Chem. C, **1**, 1197 (2013).

[6] M. Xu, J. Hu, X. Zou, S. Dong, M. Liu, X. Yang and X. Liu, J. Polym. Res. **20**, 170 (2013).

[7] A. Pratt, M. Kurahashi, X. Sun and Y. Yamauchi, J. Phys. D: Appl. Phys. **44**, 064010 (2011).

[8] J. Gass, P. Poddar, J. Almand S. Srinath, and H. Srikanth, Adv. Funct. Mater. **16**, 71 (2006).

[9] F.J. Yue, S.Wang, D. Wu, Appl Phys A **111**,347 (2013)

[10] Z. Liu, J. Wang, D. Xie, and G. Chen, Small **4**, 462 (2008).

[11] Z. Xu, Y. Hou, S. Sun, J. Am. Chem. Soc. **129**, 8698 (2007).

[12] C. Ban, Z. Wu, D.T. Gillaspie, L. Chen, Y. Yan, J. L. Blackburn, and A. C. Dillon, Adv. Mater. **22**, E145 (2010).

[13] M. Fonin, R. Pentcheva, Y.S. Dedkov, M. Sperlich, D.V. Vyalikh, M. Scheffler, U. Rüdiger, G. Güntherodt, Phys. Rev. B **72**, 104436 (2005).

[14] J.G. Tobin, S.A. Morton, S.W. Yu, G.D. Waddill, I.K. Schuller, S.A. Chambers, J. Phys.: Condens. Matter **19**, 315218 (2007).

[15] X. Sun, M. Kurahashi, A. Pratt, Y. Yamauchi, Surf. Sci. **605**, 1067 (2011).

[16] R. Pentcheva, W. Moritz, J. Rundgren, S. Frank, D. Schrupp, M. Scheffler, Surf. Sci. **602**, 1299 (2008).

[17] M. Kurahashi, X. Sun, Y. Yamauchi, Phys. Rev. B **81**, 193402 (2010).

[18] A. Pratt, M. Kurahashi, X. Sun, D. Gilks, and Y. Yamauchi, Phys. Rev. B **85**, 180490(R) (2012).

[19] G. S. Parkinson, N. Mulakaluri, Y. Losovyj, P. Jacobson, R. Pentcheva, and U. Diebold, Phys. Rev. B **82**, 125413 (2010).

[20] X. Sun, S. D. Li, B. Wang, M. Kurahashi, A. Pratt and Y. Yamauchi, Phys. Chem. Chem. Phys. **16**, **95** (2014).

[21] G. Kresse, J. Furthmüller, Phys. Rev. B **54**, 11169 (1996).

[22] G. Kresse, J. Furthmüller, Comput. Mater. Sci. **6**, 15 (1996).

[23] J. P. Perdew, K. Burke, M. Ernzerhof, Phys. Rev. Lett. **77**, 3865 (1996).

[24] G. Kresse, D. Joubert, Phys. Rev. B **59**, 1758 (1999).

[25] P. E. Blöchl, Phys. Rev. B **50**, 17953 (1994).

[26] H. J. Monkhorst and J. D. Pack, Phys. Rev. B **13**, 5188 (1976).

[27] I.V. Shvets, G. Mariotto, K. Jordan, N. Berdunov, R. Kantor, S. Murphy, Phys. Rev. B **70** , 155406(2004).

[28] Z. Lodziana, Phys. Rev. Lett. **99**, 206402 (2007).

[29] R. Pentcheva, F. Wendler, H. L. Meyerheim, W. Moritz, N. Jedrecy, and M. Scheffler, Phys. Rev. Lett. **94**, 126101 (2005).

[30] C. Cheng, Phys. Rev. B **71**, 052401 (2005).

[31] R. Bliem, E. McDermott, P. Ferstl, M. Setvin, O. Gamba, J. Pavelec, M. A. Schneider, M. Schmid, U. Diebold, P. Blaha, L. Hammer, and G. S. Parkinson, Science **346**, 1215 (2014).

	Clean Fe_3O_4	H/ Fe_3O_4	C/ Fe_3O_4	B/ Fe_3O_4
E_{ads} (eV)	-	-3.096	-5.509	-5.761
E_{M-M} (eV)	-	-0.293	-1.081	-1.844
E_{surf} (eV)	-	+0.609	+1.812	+1.121
E_{M-sub} (eV)	-	-3.412	-6.240	-5.038
$\Delta_{spin-up}$ (eV)	-	0.65	0.73	0.74
Δ_{EF-VBM} (eV)	-	0.25	0.40	0.37
$d_{Fe(B)-Fe(B)}$ (Å)	2.917	2.560	2.451	2.551
d_{O1-O1} (Å)	2.457	2.503	2.912	2.875
d_{O2-O2} (Å)	2.600	2.861	2.946	2.862
$d_{O1-Fe(B)}$ (Å)	1.956	2.116	2.327	2.266
$d_{Fe(B)-M}$ (Å)	-	2.762	2.479	2.266
d_{O1-M} (Å)	-	0.970	1.210	1.303
d_{M-M} (Å)	-	1.836	2.292	1.695
θ_{M-O1} (^{o})	-	56.3	18.1	57.9
$\theta_{Fe(B)-O1-M}$ (^{o})	-	122.6	82.5	72.0

Table 1. Calculated values for the adsorption energy (E_{ads}), adsorbate-adsorbate energy (E_{M-M}), surface modification energy (E_{surf}), adsorbate-substrate energy (E_{M-sub}), band gap and energy interval from the Fermi level (E_F) to the valence band maximum (VBM) of spin-up electronic states, the nearest distance of neighboring atoms, the tilting angle of adsorbate-O1 bonds from the surface normal, and the angle between Fe(B)-O1-M atoms for clean, H-adsorbed, C-adsorbed and B-adsorbed Fe_3O_4(100) surfaces.

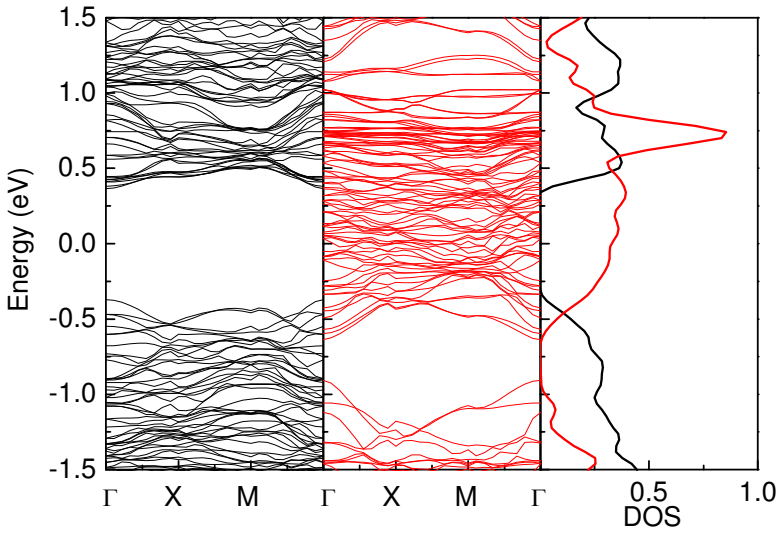

Fig. 1 Band structure (left and middle panels) and total density of states (DOS) (right panel) for the B-adsorbed Fe_3O_4(100) surface. Black and red lines represent spin-up and spin-down electronic states, respectively.

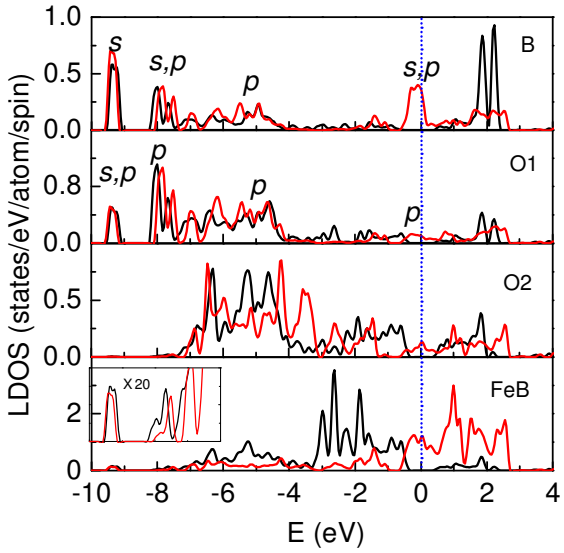

Fig. 2. Local density of states (LDOS) of Fe(B), O2, O1 and adsorbed B atoms. Black and red lines represent spin-up and spin-down electronic states, respectively.

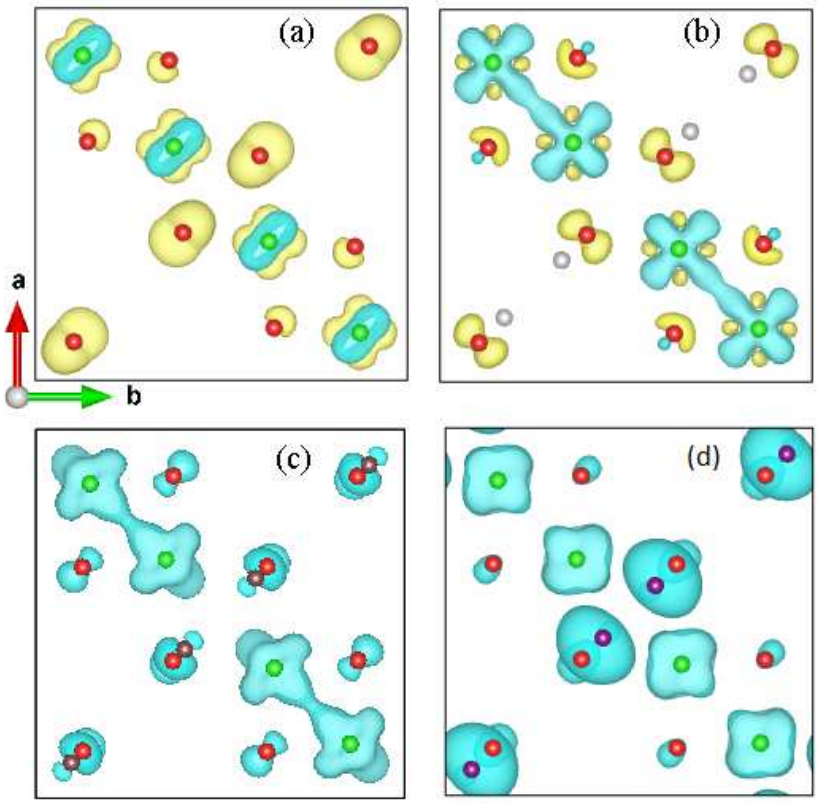

Fig. 3. Spin density of the topmost surface integrated from -0.5 eV to the Fermi level. (a) clean $Fe_3O_4(100)$, (b) H-adsorbed $Fe_3O_4(100)$, (c) C-adsorbed $Fe_3O_4(100)$ and (d) B-adsorbed $Fe_3O_4(100)$. The isosurfaces are all plotted with 0.005 eV/Å^3. Yellow and blue colors represent positive and negative spin density, respectively. Green and red spheres represent the positions of Fe(B) and O atoms located at the topmost layer of the substrate. Gray, brown and purple spheres show the positions of adsorbed of H, C and B atoms, respectively. For ease of viewing, atomic positions are shifted above the surface.

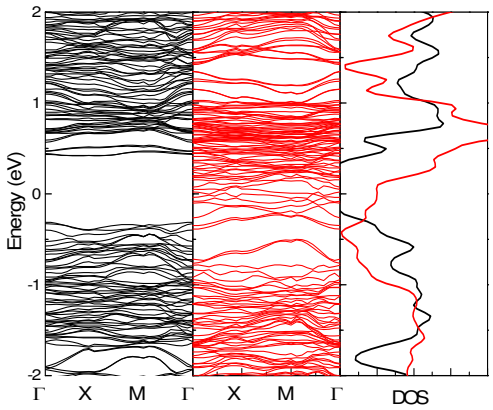

Fig. 4. Band structure (left and middle panels) and total density of states (DOS) (right panel) for B-adsorbed Fe_3O_4(100) incorporating the SCV structure using the GGA method. Black and red lines represent spin-up and spin-down electronic states, respectively.

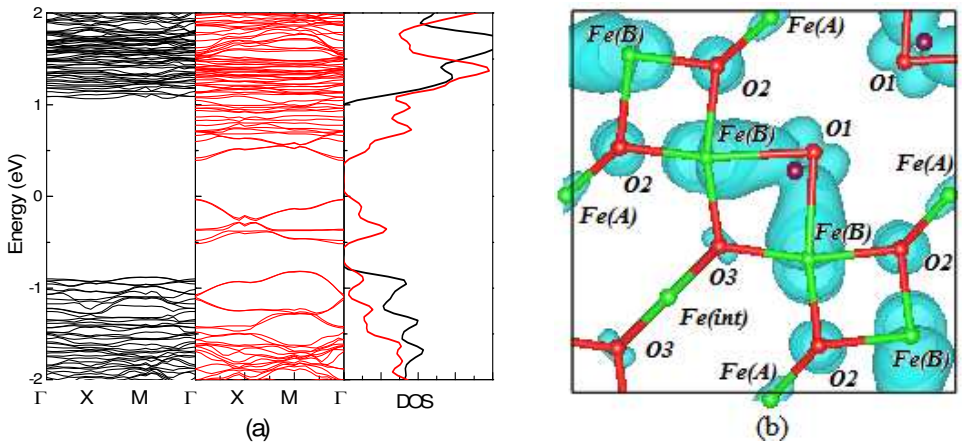

Fig. 5. Band structure (a) and spin density (b) integrated from -0.5 eV to the Fermi level for the B-adsorbed SCV Fe_3O_4(100) structure using the GGA+U method. Black and red lines in (a) represent spin-up and spin-down electronic states, respectively. Blue color in (b) represents negative spin density. Red and green sticks represent Fe-O bonds. The second layer is also shown in (b) to display the position of Fe(int) atoms.